Malaysian Journal of Mathematical Sciences 16(2): 185–197 (2022)
https://doi.org/10.47836/mjms.16.2.02

Malaysian Journal of Mathematical Sciences

Journal homepage: https://einspem.upm.edu.my/journal

Effect of Mechanical Loadings on Two Unequal Slanted Cracks Length in Bi-Materials Plate

Hamzah, K. B.[1] and Nik Long, N. M. A.*[2,3]

[1]*Fakulti Teknologi Kejuruteraan Mekanikal dan Pembuatan, Universiti Teknikal Malaysia Melaka, Malaysia*
[2]*Mathematics Department and Statistics, Faculty of Science, Universiti Putra Malaysia, Malaysia*
[3]*Laboratory of Computational Sciences and Mathematical Physics, Institute for Mathematical Research, Universiti Putra Malaysia, Malaysia*

E-mail: nmasri@upm.edu.my
**Corresponding author*

Received: 15 June 2021
Accepted: 12 July 2021

Abstract

Although a lot of crack problems in bi-materials plate were previously treated, few solutions are available under mechanical loadings, arbitrary crack lengths and material combinations. In this paper the dimensionless stress intensity factors (SIFs) of two slanted cracks in the upper plate of bi-materials are considered under mechanical loadings with varying the crack length and material combinations systematically. In order to calculate the dimensionless SIFs accurately, the hypersingular integral equations (HSIEs) was formulated by using the modified complex potentials (MCP) function. The details numerical results of the dimensionless SIFs are given in tabular form and graphical presentations. Comparisons with the existing exact solutions show that the numerical results in this paper have high accuracy. Our results are described with clarifying the effect of the mechanical loadings, bi-elastic constant ratio and element size of cracks on the dimensionless SIFs.

Keywords: bi-materials; hypersingular integral equations; slanted cracks; stress intensity factors.

1 Introduction

Bi-materials plate are widely used in mechanical parts and components working in harsh and special environments, such as mechanical, manufacturing, petrochemical industry, nuclear engineering, automotive industry, aerospace, electronic information and others because of their special properties. Due to the different materials properties of this plate, the mechanical performance of the bi-materials will be different from that of the single material under mechanical loadings. Therefore, it is of great significance to study the fracture mechanics such as crack problems in bi-materials plate under mechanical loadings because it is one of the main reasons for the failure of bi-materials structure.

Previously, the analysis of cracks in the bi-materials plate for simple geometries and mechanical loadings has been conducted by Erdogan [4] who discussed straight-line cracks, meanwhile, Hamoush and Ahmad [5] investigated a mixed-mode interface crack. Chen and Hasebe [2] presented stress intensity factors (SIFs) for a curved circular crack in bi-materials, whereas Isida and Noguchi [10] are focused on the cracks subjected to various loading. However all these solutions are for a specific geometry and mechanical loading and for a more general configuration of loading and geometries, numerical procedures are necessary to find the SIFs. Zhou et al. [20] used a system of complex Cauchy type singular integral equations to obtain the dimensionless SIFs for an arbitrary crack problems in bi-materials. Lan et al. [11] analyzed on the effect of material combinations and relative crack size to the dimensionless SIFs at the crack tip of a bi-materials. Noda and Lan [16] presented the dimensionless SIFs of an edge interface crack in bi-materials plate under tension with varying crack length and material combinations systematically. Li et al. [12] used Fourier transform technique to calculate the nondimensionless SIFs for a crack lying at the interface of bi-materials subjected to shear and compression stress. Huang et al. [9] developed a system to evaluate the mixed-mode dynamic SIFs for an interface crack in bi-materials with an inclusion close to the crack tip under an impact loading. Hamzah et al. [6] calculated the dimensionless SIFs for multiple cracks in the upper plate of bi-materials subjected to shear stress by using hypersingular integral equations (HSIEs) and modified complex potential (MCP) function. They expanded their study to analyze the behavior of dimensionless SIFs under various mechanical loadings, however focused on a single crack in the upper plate of bi-materials (Hamzah et al. [8]). Yang et al. [19] analyzed on Mode III nanocrack at the interface of bi-materials under antiplane shear loading by reducing Fourier transform problems to a set of hypersingular integro-differential equations. According to Chai et al. [1], the value of Mode I SIFs is larger than the value of Mode II SIFs for interface circular crack in bi-materials under axisymmetric loadings.

The present study is a novel investigation on two unequal slanted cracks length in the upper plate of bi-materials under shear and normal stresses for calculating the dimensionless SIFs at the crack tip. By using MCP method, the problem is formulated into HSIEs. The noticeable impact of stresses, bi-elastic constants ratio and crack geometry conditions on dimensionless SIFs for bi-materials plate have been depicted by means of numerical computations and graphical demonstrations. Moreover, a comparative analysis is carried out for dimensionless SIFs in bi-materials under shear and normal stresses to elucidate the unrevealed facts. The present findings may assist the engineers in investigating the stability behavior of the perfectly bonded bi-materials structures under various mechanical loadings.

2 Mathematical Formulation

In this section, the two unequal slanted cracks length in the upper plate of bi-materials under shear and normal stresses is studied. The problem is formulated into the systems of HSIEs using the MCP method, and with the help of the continuity conditions of the resultant force function and displacement. The appropriate quadrature formulas are used to solve numerically the unknown COD function and the traction along the crack as the right hand term of HSIEs.

2.1 Complex Potential Function (CPF)

Muskhelishvili [14] introduced the CPF method which plays an important role in solving the cracks problems in elasticity plate. In this method, the stress components $(\sigma_x, \sigma_y, \sigma_{xy})$, resultant force function $f(X, Y)$ and displacements (u, v) are related to two principal parts of the CPF $\phi_{1p}(z)$ and $\psi_{1p}(z)$ in terms of $z = x + iy$ as follows:

$$\sigma_y - \sigma_x + 2i\sigma_{xy} = 2[\bar{z}\phi''_{1p}(z) + \psi'_{1p}(z)], \tag{1}$$

$$f = -Y + iX = \phi_{1p}(z) + z\overline{\phi'_{1p}(z)} + \overline{\psi_{1p}(z)}, \tag{2}$$

$$2G(u + iv) = \kappa\phi_{1p}(z) - z\overline{\phi'_{1p}(z)} - \overline{\psi_{1p}(z)}, \tag{3}$$

where G is shear modulus of elasticity, $\kappa = (3 - v)/(1 + v)$ for plane stress, $\kappa = 3 - 4v$ for plane strain and v is Poisson's ratio. Then, the derivative of Equation (2) with respect to z give the results interms of normal, $N(z)$, and tangential, $T(z)$, components as follows:

$$\frac{d}{dz}\big(-Y + iX\big) = \phi'_{1p}(z) + \overline{\phi'_{1p}(z)} + \left(z\overline{\phi''_{1p}(z)} + \overline{\psi'_{1p}(z)}\right)\frac{d\bar{z}}{dz} = N(z) + iT(z). \tag{4}$$

Note that the traction $N(z) + iT(z)$ depends on the position of point z and the direction of the segment $d\bar{z}/dz$.

Based on studied by Nik Long and Eshkuvatov [15], the CPF for a crack L in an infinite plate can be expressed by

$$\phi_{1p}(z) = \frac{1}{2\pi}\int_L \frac{g(t)dt}{t - z}, \tag{5}$$

$$\psi_{1p}(z) = \frac{1}{2\pi}\int_L \frac{g(t)d\bar{t}}{t - z} + \frac{1}{2\pi}\int_L \frac{\overline{g(t)}dt}{t - z} - \frac{1}{2\pi}\int_L \frac{\bar{t}g(t)dt}{(t - z)^2}, \tag{6}$$

where $g(t)$ is COD function denoted by the displacements at point t of the upper, $(u(t) + iv(t))^+$, and lower, $(u(t) + iv(t))^-$, crack faces as follows

$$g(t) = \frac{2G}{i(\kappa + 1)}\Big((u(t) + iv(t))^+ - (u(t) + iv(t))^-\Big). \tag{7}$$

Note that at the crack tip A_j, $g(t)$ has the following properties

$$g(t) = O\left(\sqrt{t - t_{A_j}}\right) \tag{8}$$

where $j = 1, 2$.

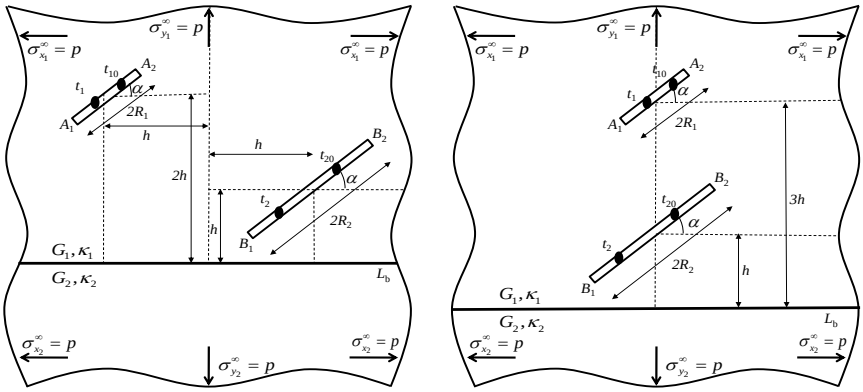

Figure 1: Two unequal slanted cracks length in the upper plate of bi-materials under shear and normal stresses. Left) In series; Right) In parallel.

2.2 Bi-Materials Plate

Consider two unequal slanted cracks length in the upper plate of bi-materials under shear and normal stresses as shows in Figure 1. The conditions for strain components ε in bi-materials can be defined by Young's modulus of elasticity E and stress components σ as follows

$$\varepsilon_{x_j} = \frac{1}{E_j}\left(\sigma^{\infty}_{x_j} - v_j\sigma^{\infty}_{y_j}\right), \qquad \varepsilon_{y_j} = \frac{1}{E_j}\left(\sigma^{\infty}_{y_j} - v_j\sigma^{\infty}_{x_j}\right), \tag{9}$$

where $j = 1, 2$ are the strain components for the upper and lower plates of bi-materials, respectively, and $E_j = 2G_j(1 + v_j)$. By assuming the others mechanical loadings do not exist, then the shear stress is reduced to

$$\frac{1}{E_1}\sigma^{\infty}_{x_1} = \frac{1}{E_2}\sigma^{\infty}_{x_2}. \tag{10}$$

Similar conditions for normal stress is reduced to

$$\frac{1}{E_1}\sigma^{\infty}_{y_1} = \frac{1}{E_2}\sigma^{\infty}_{y_2}. \tag{11}$$

According to Hamzah et al. [7], if the shear stress $\sigma_{x_1} = \sigma_{x_2} = p$ and normal stress $\sigma_{y_1} = \sigma_{y_2} = p$ then $N(z) + iT(z)$ are defined as follows

$$N(z) + iT(z) = -p\sin^2\alpha - ip\sin\alpha\cos\alpha, \tag{12}$$

$$N(z) + iT(z) = -p\cos^2\alpha + ip\sin\alpha\cos\alpha, \tag{13}$$

where α is an angle of the crack.

Studied by Chen and Hasebe [2], the MCPs for a crack in the upper plate of bi-materials are defined as follows

$$\phi_1(z) = \phi_{1p}(z) + \phi_{1c}(z), \qquad \psi_1(z) = \psi_{1p}(z) + \psi_{1c}(z), \tag{14}$$

where $\phi_{1c}(z)$ and $\psi_{1c}(z)$ are the complementary parts of the CPF. Then the CPF for the lower plate of bi-materials are represented by $\phi_2(z)$ and $\psi_2(z)$. By applying continuity conditions between upper and lower plates of bi-materials, Equations (2) and (3) gives

$$\left(\phi_1(t) + t\overline{\phi_1'(t)} + \overline{\psi_1(t)}\right)^+ = \left(\phi_2(t) + t\overline{\phi_2'(t)} + \overline{\psi_2(t)}\right)^-, \tag{15}$$

$$G_2\left(\kappa_1\phi_1(t) - t\overline{\phi_1'(t)} - \overline{\psi_1(t)}\right)^+ = G_1\left(\kappa_2\phi_2(t) - t\overline{\phi_2'(t)} - \overline{\psi_2(t)}\right)^-, \tag{16}$$

where $t \in L_j$, $j = 1, 2$, and $+$ and $-$ sign represent the upper and lower plates of bi-materials, respectively. Substitute Equation (14) into Equations (15) and (16), it will reduces to the following equations

$$\phi_{1c}(z) = \Lambda_1\left(z\overline{\phi_{1p}'}(z) + \overline{\psi_{1p}}(z)\right), \quad z \in S_1 + L_b, \tag{17}$$

$$\psi_{1c}(z) = \Lambda_2\overline{\phi_{1p}}(z) - \Lambda_1\left(z\overline{\phi_{1p}'}(z) + z^2\overline{\phi_{1p}''}(z) + z\overline{\psi_{1p}'}(z)\right), \quad z \in S_1 + L_b, \tag{18}$$

$$\phi_2(z) = \Lambda_2\phi_{1p}(z) + \phi_{1p}(z), \quad z \in S_2 + L_b, \tag{19}$$

$$\psi_2(z) = \Lambda_1\left(z\phi_{1p}'(z) + \psi_{1p}\right) - \Lambda_2 z\phi_{1p}'(z) + \psi_{1p}, \quad z \in S_2 + L_b, \tag{20}$$

where $\overline{\phi_{1p}}(z) = \overline{\phi_{1p}(\bar{z})}$. Note that L_b is boundary of bi-materials, S_1 and S_2 are upper and lower plates of bi-materials, respectively, and Λ_1 and Λ_2 are bi-elastic constants defined as

$$\Lambda_1 = \frac{G_2 - G_1}{G_1 + \kappa_1 G_2}, \qquad \Lambda_2 = \frac{\kappa_1 G_2 - \kappa_2 G_1}{G_2 + \kappa_2 G_1}.$$

2.3 Hypersingular Integral Equations (HSIEs)

The HSIEs for two unequal slanted cracks length in the upper plate of bi-materials under shear and normal loadings can be formulated by defining four traction components $\left(N(t_{10})+iT(t_{10})\right)_{11}$, $\left(N(t_{10})+iT(t_{10})\right)_{12}$, $\left(N(t_{20})+iT(t_{20})\right)_{22}$ and $\left(N(t_{20})+iT(t_{20})\right)_{21}$ which consist of two groups of $N(t_{j0}) + iT(t_{j0})$, $(j = 1, 2)$. The first group involve $\left(N(t_{10}) + iT(t_{10})\right)_{11}$ and $\left(N(t_{20}) + iT(t_{20})\right)_{21}$ that obtained from reaction between $g_1(t_1)$ at $t_1 \in L_1$ and the observation point placed at $t_{10} \in L_1$ and $t_{20} \in L_2$. However, the second group involve $\left(N(t_{10})+iT(t_{10})\right)_{12}$ and $\left(N(t_{20})+iT(t_{20})\right)_{22}$ that obtained from reaction between $g_2(t_2)$ at $t_2 \in L_2$ and the observation point is placed at $t_{10} \in L_1$ and $t_{20} \in L_2$. Since both unequal slanted cracks length lie in the upper plate of bi-materials, we need to combine four traction components which consist of principal, $\left(N(t_{j0}) + iT(t_{j0})\right)_{jp}$ and complementary parts, $\left(N(t_{j0}) + iT(t_{j0})\right)_{jc}$, then the HSIEs can be obtained as follows:

$$\begin{aligned}\big(N(t_{10})+iT(t_{10})\big)_1 &= \big(N(t_{10})+iT(t_{10})\big)_{11}+\big(N(t_{10})+iT(t_{10})\big)_{12}\\ &= \frac{1}{\pi}\neq\!\!\!\!\!\!\int_{L_1}\frac{g_1(t_1)dt_1}{(t_1-t_{10})^2}+\frac{1}{2\pi}\int_{L_1}D_1(t_1,t_{10})g_1(t_1)dt_1\\ &+\frac{1}{2\pi}\int_{L_1}D_2(t_1,t_{10})\overline{g_1(t_1)}dt_1+\frac{1}{\pi}\int_{L_2}\frac{g_2(t_2)dt_2}{(t_2-t_{10})^2}\\ &+\frac{1}{2\pi}\int_{L_2}D_1(t_2,t_{10})g_2(t_2)dt_2+\frac{1}{2\pi}\int_{L_2}D_2(t_2,t_{10})\overline{g_2(t_2)}dt_2,\end{aligned}\tag{21}$$

$$\begin{aligned}\big(N(t_{20})+iT(t_{20})\big)_2 &= \big(N(t_{20})+iT(t_{20})\big)_{22}+\big(N(t_{20})+iT(t_{20})\big)_{21}\\ &= \frac{1}{\pi}\neq\!\!\!\!\!\!\int_{L_2}\frac{g_2(t_2)dt_2}{(t_2-t_{20})^2}+\frac{1}{2\pi}\int_{L_2}D_1(t_2,t_{20})g_2(t_2)dt_2\\ &+\frac{1}{2\pi}\int_{L_2}D_2(t_2,t_{20})\overline{g_2(t_2)}dt_2+\frac{1}{\pi}\int_{L_1}\frac{g_1(t_1)dt_1}{(t_1-t_{20})^2}\\ &+\frac{1}{2\pi}\int_{L_1}D_1(t_1,t_{20})g_1(t_1)dt_1+\frac{1}{2\pi}\int_{L_1}D_2(t_1,t_{20})\overline{g_1(t_1)}dt_1,\end{aligned}\tag{22}$$

where

$$\begin{aligned}D_1(t_{\rm i},t_{\rm j0}) &= \Lambda_1\bigg(\frac{1}{(t_{\rm i}-\bar{t}_{\rm j0})^2}+\frac{2(\bar{t}_{\rm j0}-\bar{t}_{\rm i})}{(t_{\rm i}-\bar{t}_{\rm j0})^3}-\frac{d\bar{t}_{\rm j0}}{dt_{\rm j0}}\bigg(\frac{1}{(t_{\rm i}-\bar{t}_{\rm j0})^2}-\frac{2(2t_{\rm j0}-3\bar{t}_{\rm j0}+\bar{t}_{\rm i})}{(t_{\rm i}-\bar{t}_{\rm j0})^3}\\ &-\frac{6(\bar{t}_{\rm j0}-\bar{t}_{\rm i})(\bar{t}_{\rm j0}-t_{\rm j0})}{(t_{\rm i}-\bar{t}_{\rm j0})^4}\bigg)\bigg)-\Lambda_1\bigg(\frac{d\bar{t}_{\rm j0}}{dt_{\rm j0}}\bigg(\frac{1}{(t_{\rm i}-\bar{t}_{\rm j0})^2}+\frac{2(\bar{t}_{\rm j0}-t_{\rm j0})}{(t_{\rm i}-\bar{t}_{\rm j0})^3}\bigg)\\ &-\frac{1}{(\bar{t}_{\rm i}-t_{\rm j0})^2}-\frac{1}{(t_{\rm i}-\bar{t}_{\rm j0})^2}\bigg)\frac{d\bar{t}_{\rm i}}{dt_{\rm i}}+\frac{1}{(t_{\rm i}-t_{\rm j0})^2}\bigg(\frac{(t_{\rm i}-t_{\rm j0})^2}{(\bar{t}_{\rm i}-\bar{t}_{\rm j0})^2}\frac{d\bar{t}_{\rm i}}{dt_{\rm i}}\frac{d\bar{t}_{\rm j0}}{dt_{\rm j0}}-1\bigg)\\ &+\Lambda_2\frac{d\bar{t}_{\rm j0}}{dt_{\rm j0}}\frac{1}{(t_{\rm i}-\bar{t}_{\rm j0})^2},\end{aligned}$$

$$\begin{aligned}D_2(t_{\rm i},t_{\rm j0}) &= \Lambda_1\bigg(\frac{1}{(\bar{t}_{\rm i}-t_{\rm j0})^2}+\frac{1}{(t_{\rm i}-\bar{t}_{\rm j0})^2}-\frac{d\bar{t}_{\rm j0}}{dt_{\rm j0}}\bigg(\frac{1}{(t_{\rm i}-\bar{t}_{\rm j0})^2}+\frac{2(\bar{t}_{\rm j0}-t_{\rm j0})}{(t_{\rm i}-\bar{t}_{\rm j0})^3}\bigg)\bigg)\\ &+\Lambda_1\bigg(\frac{1}{(\bar{t}_{\rm i}-t_{\rm j0})^2}+\frac{2(t_{\rm j0}-t_{\rm i})}{(\bar{t}_{\rm i}-t_{\rm j0})^3}\bigg)\frac{d\bar{t}_{\rm i}}{dt_{\rm i}}-\frac{t_{\rm i}-t_{\rm j0}}{(\bar{t}_{\rm i}-\bar{t}_{\rm j0})^3}\bigg(2\frac{d\bar{t}_{\rm i}}{dt_{\rm i}}\frac{d\bar{t}_{\rm j0}}{dt_{\rm j0}}\\ &-\frac{(\bar{t}_{\rm i}-\bar{t}_{\rm j0})}{(t_{\rm i}-t_{\rm j0})}\bigg(\frac{d\bar{t}_{\rm i}}{dt_{\rm i}}+\frac{d\bar{t}_{\rm j0}}{dt_{\rm j0}}\bigg)\bigg),\end{aligned}$$

and $i,j=1,2$. Note that the first integral with the equal sign in Equations (21) and (22) represents the hypersingular integral and must be defined as a finite part integral. If $G_2=0$, then Equations (21) and (22) reduce to the HSIEs for the two unequal slanted cracks length in a half plate, refer Chen et al. [3]. Whereas, if $G_1=G_2$, then Equations (21) and (22) reduce to the HSIEs for the two unequal slanted cracks length in an infinite plate, refer Nik Long and Eshkuvatov [15].

2.4 Dimensionless Stress Intensity Factors

The curved length coordinate method is used to solve the HSIEs for two unequal slanted cracks length in the upper plate of bi-materials under shear and normal loadings. After that, the quadrature formulas introduced by Mayrhofer and Fischer [13] can be applied. In order to investigate the behavior of dimensionless SIFs for two unequal slanted cracks length in the upper plate of bi-materials under shear and normal loadings, we define the SIFs at the crack tips A_j and B_j $(j = 1, 2)$ as follows

$$K_{A_j} = (K_1 - iK_2)_{A_j} = \sqrt{2\pi} \lim_{t \to t_{A_j}} \sqrt{|t - t_{A_j}|} g_1'(t_1), \tag{23}$$

$$K_{B_j} = (K_1 - iK_2)_{B_j} = \sqrt{2\pi} \lim_{t \to t_{B_j}} \sqrt{|t - t_{B_j}|} g_2'(t_2), \tag{24}$$

where K_1 and K_2 are opening and sliding modes, respectively, and $g_1'(t_1)$ and $g_2'(t_2)$ are defined as follows

$$g_k'(t_k)|_{t_k = t_k(s_k)} = \frac{-s_k H_k(s_k)}{\sqrt{a_k^2 - s_k^2}} e^{-i\theta_{A_j}}, \qquad H_k'(s_k) = 0, \tag{25}$$

and $k = 1, 2$.

Therefore the dimensionless SIFs at crack tips A_j and B_j are defined as follows

$$K_{A_j} = \sqrt{2\pi} \lim_{s \to s_{A_j}} \sqrt{|s - s_{A_j}|} \left(\frac{-s_1 H_1(s_1)}{\sqrt{a_1^2 - s_1^2}} e^{-i\theta_{A_j}} \right) = \sqrt{a_1 \pi} F_{A_j}, \tag{26}$$

$$K_{B_j} = \sqrt{2\pi} \lim_{s \to s_{B_j}} \sqrt{|s - s_{B_j}|} \left(\frac{-s_2 H_2(s_2)}{\sqrt{a_2^2 - s_2^2}} e^{-i\theta_{B_j}} \right) = \sqrt{a_2 \pi} F_{B_j}, \tag{27}$$

where

$$F_{A_j} = H_1(-a_1) e^{-i\theta_{A_j}} = F_{1A_j} + iF_{2A_j},$$
$$F_{B_j} = H_2(-a_2) e^{-i\theta_{B_j}} = F_{1B_j} + iF_{2B_j}.$$

F_{1A_j} and F_{1B_j} are the Mode I dimensionless SIFs at crack tips A_j and B_j, respectively, and characterizes the amplitude of normal stress singularity. Whereas F_{2A_j} and F_{2B_j} are the Mode II dimensionless SIFs at crack tips A_j and B_j, respectively, and describe the amplitude of the shear stress singularity. According to Petersen [17], the crack propagates if the value of dimensionless SIFs is greater than or equals to value of critical dimensionless SIFs. Wang [18] pointed out that the strength of the materials is getting weaker as the value of dimensionless SIFs increases.

3 Numerical Results and Discussion

In this section, numerical computations and graphical demonstrations are carried out to show the effects of the mechanical loadings, bi-elastic constant ratio and geometry conditions on the dimensionless SIFs for crack problems in the upper plate of bi-materials.

The numerical results have been compared with existing results studied by Isida and Noguchi [10] to illustrate efficiency of this approach for a crack problem in bi-materials plate subjected to normal stress and $G_2/G_1 = 0.5$ as shown in Table 1. The results show negligible difference between the results of the present study and those obtained by Isida and Noguchi [10]. We observed that F_{1A_1} is equal to F_{1A_2}, however F_{2A_1} is equal to the negative of F_{2A_2}. This is due to the equivalence of the stress acting at the tips of the cracks.

Table 1: Comparison between the numerical results of the present study and the results of Isida and Noguchi [10].

SIF	$h/2R$					
	0.1	0.2	0.3	0.4	0.5	0.6
${F_{1A_1}}^*$	1.1765	1.1522	1.1295	1.1083	1.0899	1.0745
${F_{2A_1}}^*$	-0.0951	-0.0721	-0.0562	-0.0428	-0.0322	-0.0241
${F_{1A_2}}^*$	1.1765	1.1522	1.1295	1.1083	1.0899	1.0745
${F_{1A_2}}^{**}$	1.1760	1.1520	1.1300	1.1080	1.0900	1.0750
${F_{2A_2}}^*$	0.0951	0.0721	0.0562	0.0428	0.0322	0.0241
${F_{2A_2}}^{**}$	0.0950	0.0720	0.0560	0.0430	0.0320	0.0240

*Present study, **Isida and Noguchi[10]

In the following discussion, we evaluate the example with two unequal slanted cracks length in series in the upper plate of bi-materials under shear and normal stresses as defined in Figure 1 (left).

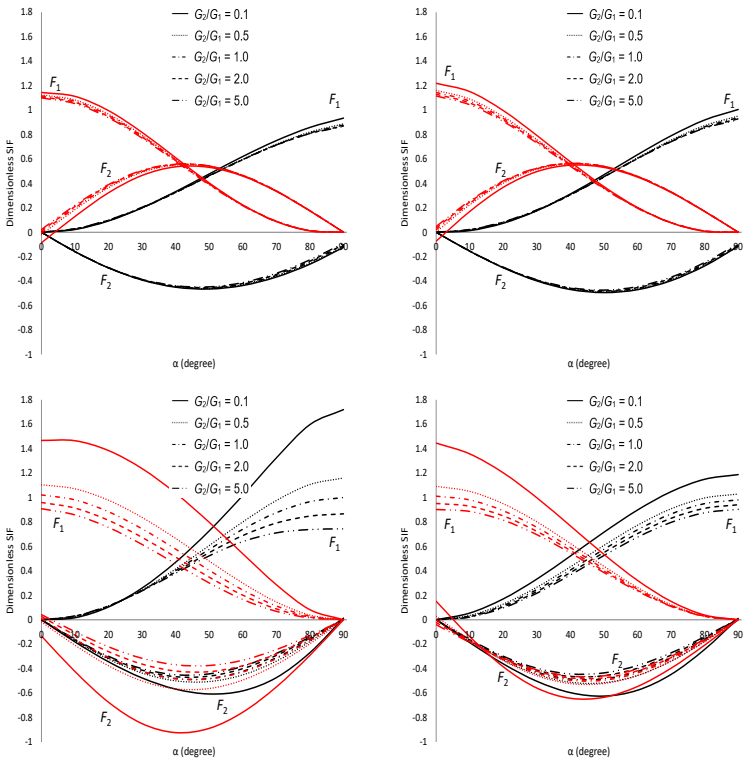

Figure 2: Dimensionless SIFs for two unequal slanted cracks length in the upper plate of bi-materials under shear (black line) and normal (red line) stresses. Top Left: Crack tip A_1; Top Right: Crack tip A_2; Bottom Left: Crack tip B_1; Bottom Right: Crack tip B_2.

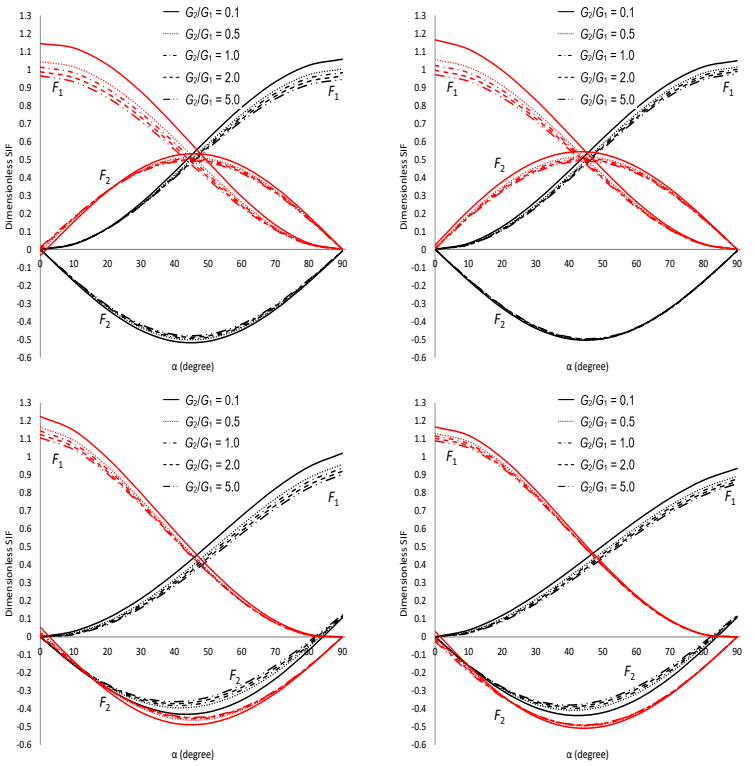

Figure 3: Dimensionless SIFs for two unequal slanted cracks length in the upper plate of bi-materials under shear (black line) and normal (red line) stresses. Top Left: Crack tip A_1; Top Right: Crack tip A_2; Bottom Left: Crack tip B_1; Bottom Right: Crack tip B_2.

The bi-materials plate have two slanted cracks with length $R_2 = 3R_1$, $R_2/h = 0.9$ and α varies. Figure 2 illustrates the effect of the mechanical loadings which is shear (black line) and normal (red line) stresses, and bi-elastic constant ratio G_2/G_1 on the dimensionless SIFs. It is obvious as α increases the dimensionless SIFs, F_1 increases with the loading of shear stress (black line) but decreases with the loading of normal stress (red line) at all crack tips. However, the increases of G_2/G_1 will decrease value of F_1 at all crack tips for both mechanical loadings. In other words, additing the shear modulus of elasticity (G_2) in the lower plate is an efficient way to reduce the dimensionless SIFs at all crack tips. If the length of slanted crack near to the boundary of bi-materials is shorter then the other crack which is $R_1 = 3R_2$ and $R_1/h = 0.9$, then the dimensionless SIFs is depicted in Figure 3. This results reveal that the dimensionless SIFs at all crack tips have similar trend with the previous example.

However, it is much clearer to compare the dimensionless SIFs for a slanted crack having longer length. Figure 4 shows that, for the shear stress, regardless of the position of cracks, a crack with longer length has the dimensionless SIFs of Mode I, F_1, higher than a crack with shorter length. Whereas, for the normal stress, regardless of the size, the dimensionless SIFs depends on the angle, α, of the cracks. As α increases the dimensionless SIFs decreases for both cracks, A and B.

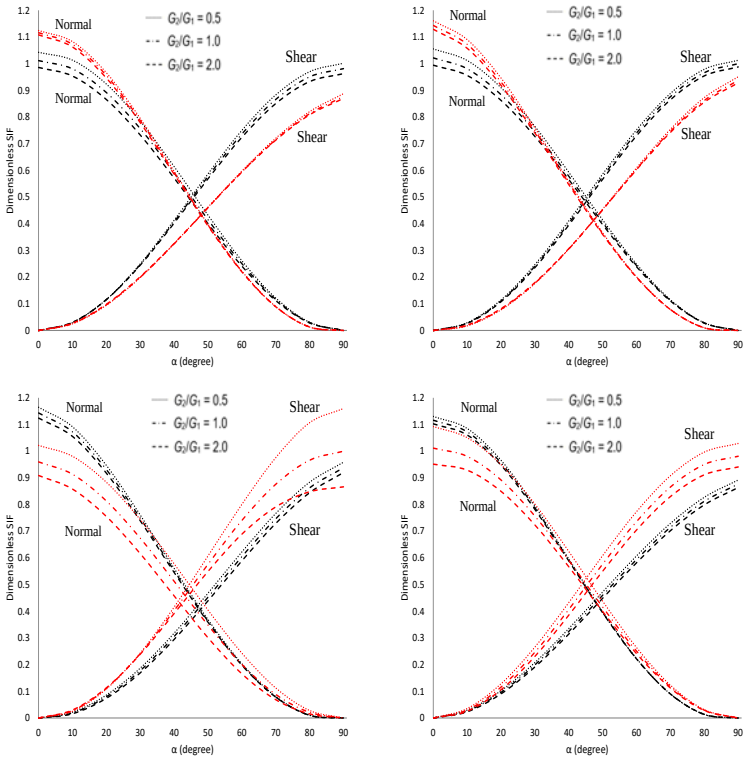

Figure 4: Comparison of the dimensionless SIFs for a slanted crack having longer length at crack A compare to B (black line) and longer length at crack B compare to A (red line) in the upper plate of bi-materials under shear and normal stresses. Top Left: Crack tip A_1; Top Right: Crack tip A_2; Bottom Left: Crack tip B_1; Bottom Right: Crack tip B_2.

In the following discussion, we evaluate the example with two unequal slanted cracks length in parallel in the upper plate of bi-materials under shear and normal stresses as defined in Figure 1 (right). The bi-materials plate have two slanted cracks with length $R_2 = 3R_1$, $R_2/h = 0.9$ and α varies. Figure 5 illustrates the variation of the peak of dimensionless SIFs versus α for five different bi-elastic constant ratios under shear (black line) and normal (red line) stresses. It is worth to mention that the dimensionless SIFs, F_1 for each crack tips reduces as the bi-elastic constant ratio, G_2/G_1 increases. For shear stress, the value of F_1 at all crack tips increases by the increases of α because of the crack growth opposites to the direction of shear stress. However for normal stress, the value of F_1 at all crack tips decreases by the increases of α because of the crack growth is similar to the direction of normal stress.

Figure 6 indicates the comparison of dimensionless SIFs for a slanted crack having longer length. It is found that, for the normal stress, regardless of the position of cracks, a crack with longer length has the dimensionless SIFs of Mode I, F_1, higher than a crack with shorter length. Whereas, for the shear stress, regardless of the position of cracks, a crack with shorter length has the dimensionless SIFs of Mode I, F_1, higher than a crack with longer length.

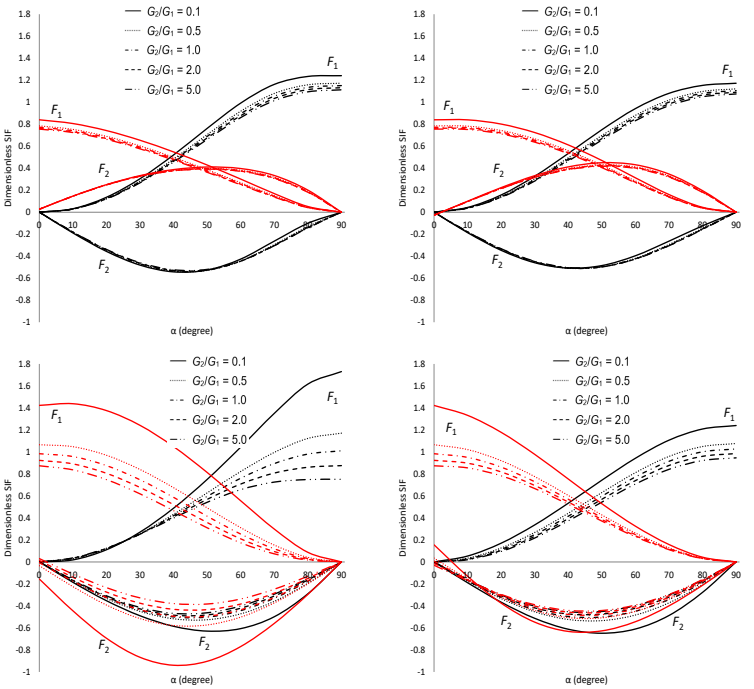

Figure 5: Dimensionless SIFs for two unequal slanted cracks length in the upper plate of bi-materials under shear (black line) and normal (red line) stresses. Top Left: Crack tip A_1; Top Right: Crack tip A_2; Bottom Left: Crack tip B_1; Bottom Right: Crack tip B_2.

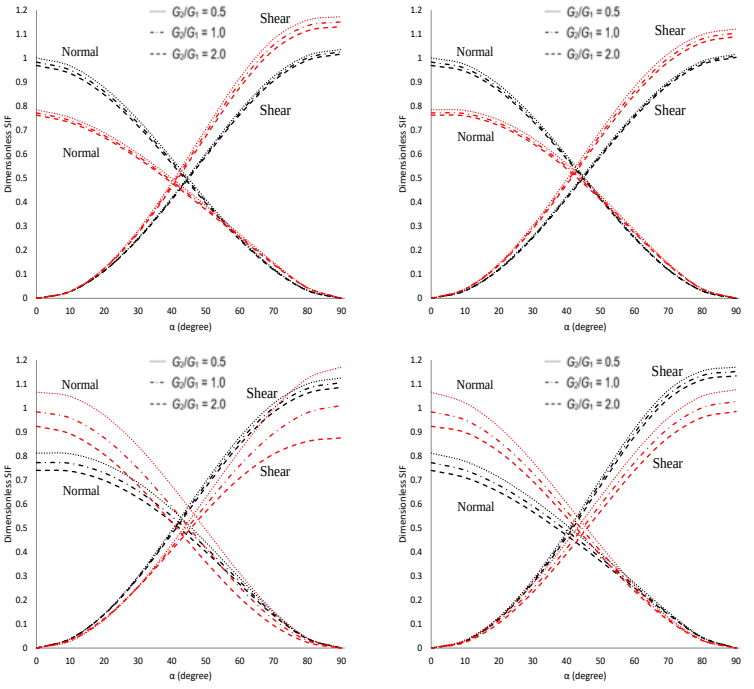

Figure 6: Comparison of the dimensionless SIFs for a slanted crack having longer length at crack A compare to B (black line) and longer length at crack B compare to A (red line) in the upper plate of bi-materials under shear and normal stresses. Top Left: Crack tip A_1; Top Right: Crack tip A_2; Bottom Left: Crack tip B_1; Bottom Right: Crack tip B_2.

4 Conclusions

In the present study, two unequal slanted cracks length in the upper plate of bi-materials under shear and normal stresses is studied using the MCP method. The continuity conditions of the resultant force and displacement were derived in terms of the COD function. The problem was reduced to a set of HSIEs in the domain under consideration, and these equations are solved numerically using the curved length coordinate method and the appropriate quadrature formulas. We can conclude that for the discussed problem, the dimensionless SIFs depends on size, cracks positions, type of mechanical loadings and bi-elastic constant ratio, and hence influence the strength of the materials. In continuation of the present study, three-dimensional crack problems in bi-materials under various mechanical loadings can be analyzed.

Acknowledgement Second author acknowledges the support from Fundamental Research Grant Scheme (FRGS) by the Ministry of Higher Education Malaysia (FRGS/1/ 2019/STG06/UPM/02/5, vote no: 5540269). The authors would like to thanks the Universiti Putra Malaysia (UPM) and Universiti Teknikal Malaysia Melaka (UTeM).

Conflicts of Interest The authors declare no conflict of interest.

References

[1] H. Chai, Y. Bao & Z. Zhang (2021). Numerical solutions of hypersingular integral equations for interface circular crack under axisymmetric loadings. *Engineering Analysis with Boundary Elements*, *122*, 35–42. https://doi.org/10.1016/j.enganabound.2020.09.016.

[2] Y. Z. Chen & N. Hasebe (1992). Stress-intensity factors for curved circular crack in bonded dissimilar materials. *Theoretical and Applied Fracture Mechanics*, *17*(3), 189–196. https://doi.org/10.1016/0167-8442(92)90027-U.

[3] Y. Z. Chen, X. Y. Lin & X. Z. Wang (2009). Numerical solution for curved crack problem in elastic half-plane using hypersingular integral equation. *Philosophical Magazine*, *89*(26), 2239–2253. https://doi.org/10.1080/14786430903032555.

[4] F. Erdogan (1963). Stress distribution in a nonhomogeneous elastic plane with cracks. *Journal of Applied Mechanics*, *30*(2), 232–236. https://doi.org/10.1115/1.3636517.

[5] S. A. Hamoush & S. H. Ahmad (1989). Mode I and mode II stress intensity factors for interfacial cracks in bi-material media. *Engineering Fracture Mechanics*, *33*(3), 421–427. https://doi.org/10.1016/0013-7944(89)90091-X.

[6] K. B. Hamzah, N. M. A. Nik Long, N. Senu & Z. K. Eshkuvatov (2019). Stress intensity factor for multiple cracks in bonded dissimilar materials using hypersingular integral equations. *Applied Mathematical Modelling*, *73*, 95–108. https://doi.org/10.1016/j.apm.2019.04.002.

[7] K. B. Hamzah, N. M. A. Nik Long, N. Senu & Z. K. Eshkuvatov (2021). Numerical solution for crack phenomenon in dissimilar materials under various mechanical loadings. *Symmetry*, *13*(2), 235–255. https://doi.org/10.3390/sym13020235.

[8] K. Hamzah, N. Nik Long, N. Senu, Z. Eshkuvatov & M. Ilias (2019). Stress intensity factors for a crack in bonded dissimilar materials subjected to various stresses. *Universal Journal of Mechanical Engineering*, *2019*(7), 179–189. http://doi.org/10.13189/ujme.2019.070405.

[9] K. Huang, L. Guo & H. Yu (2018). Investigation on mixed-mode dynamic stress intensity factors of an interface crack in bi-materials with an inclusion. *Composite Structures*, *202*, 491–499. https://doi.org/10.1016/j.compstruct.2018.02.078.

[10] M. Isida & H. Noguchi (1993). Arbitrary array of cracks in bonded half planes subjected to various loadings. *Engineering Fracture Mechanics*, *46*(3), 365–380. https://doi.org/10.1016/0013-7944(93)90230-P.

[11] X. Lan, N. A. Noda, K. Mithinaka & Y. Zhang (2011). The effect of material combinations and relative crack size to the stress intensity factors at the crack tip of a bi-material bonded strip. *Engineering Fracture Mechanics*, *78*(14), 2572–2584. https://doi.org/10.1016/j.proeng.2011.04.174.

[12] X. F. Li, G. J. Tang, Z. B. Shen & K. Y. Lee (2015). Interface crack embedded in a bi-material plane under shear and compression. *Mechanics of Materials*, *85*, 80–93. https://doi.org/10.1016/j.mechmat.2015.02.015.

[13] K. Mayrhofer & F. D. Fischer (1992). Derivation of a new analytical solution for a general two-dimensional finite-part integral applicable in fracture mechanics. *International Journal for Numerical Methods in Engineering*, *33*(5), 1027–1047. https://doi.org/10.1002/nme.1620330509.

[14] N. I. Muskhelishvili (1953). *Some basic problems of the mathematical theory of elasticity*. Noordhoff International Publishing, Leyden.

[15] N. M. A. Nik Long & Z. K. Eshkuvatov (2009). Hypersingular integral equation for multiple curved cracks problem in plane elasticity. *International Journal of Solids and Structures*, *46*(13), 2611–2617. https://doi.org/10.1016/j.ijsolstr.2009.02.008.

[16] N. A. Noda & X. Lan (2012). Stress intensity factors for an edge interface crack in a bonded semi-infinite plate for arbitrary material combination. *International Journal of Solids and Structures*, *49*(10), 1241–1251. https://doi.org/10.1016/j.ijsolstr.2012.02.001.

[17] R. C. Petersen (2013). Accurate critical stress intensity factor Griffith crack theory measurements by numerical techniques. *SAMPE Journal Society for the Advancement of Material and Process Engineering*, *2013*, 737–752.

[18] T. C. Wang (2003). Fundamentals of interface mechanics. *Reference Module in Materials Science and Materials Engineering*, *2003*, 89–135.

[19] Y. Yang, Z.-L. Hu & X.-F. Li (2020). Nanoscale mode-III interface crack in a bimaterial with surface elasticity. *Mechanics of Materials*, *140*, 103246. https://doi.org/10.1016/j.mechmat.2019.103246.

[20] Y. Zhou, X. Li & D. H. Yu (2008). Integral method for contact problem of bonded plane material with arbitrary cracks. *CMES: Computer Modeling in Engineering & Sciences*, *36*(2), 147–172. https://doi.org/10.3970/cmes.2008.036.147.